Available online www.ejaet.com

European Journal of Advances in Engineering and Technology, 2021, 8(4):1-9

Research Article **ISSN: 2394 - 658X**

Investigation of the patterns of the aerosol loads over Albania

Edmond LUKAJ[1], Florian MANDIA[2] and Floran VILA[1]

[1]Department of Physics, UniversityofTirana,Tirana,Albania - 1001
[2]Department of Physics, University of Shkodra "Luigj Gurakuqi",Shkoder, Albania - 4001
florian.mandija@unishk.edu.al

ABSTRACT
Aerosol load over Albania region was studied in this paper. Principal optical characteristics of aerosols such are aerosol optical depth and Angstrom exponent are used for this purpose. Data are retrieved basically from satellite-based observations. Principal analyses are focused over spatial and temporal distribution of these aerosol parameters, their seasonal and interannual patterns, and fine/coarse mode investigation. The overall results show that western part of Albania has the highest aerosol presence, mainly constituted by fine or mixed aerosol modes. The spring-summer period is characterized by the highest aerosol load.

Key words: Aerosol load, model-satellite data, Albania region

INTRODUCTION

Aerosols play an important role in the air quality and climate variability [1]. Aerosols contribute to the global radiation budged through their direct and indirect effects. Direct effects of aerosols imply their role on scattering-absorbing incoming-outgoing radiation [2], [3]. Meanwhile, aerosol indirect effect or aerosol cloud interactions, modulate the global radiation budged through their modification of the cloud micro-physical and geometrical properties [4]. These implications of the aerosols make them an essential factor on climate change assessments [5]. Aerosol-radiation interactions generally diminish heatwave extremes because of the reduction of the incoming solar radiation. Aerosols can change the properties of clouds, influencing to a large extent the precipitation-forming processes [6]. Their concentrations are highly inhomogeneous, and their role in climate has more regional character [7]. The presence of the aerosols also impacts the human's health [8], [9],[10].

Desert dust, or mineral dust, constitutes the major part of the natural aerosols with 60-200 million of tons per year [11], [12]. Principal sources are the major deserts, such are Sahara, Gobi, Arabian, etc. These events affect mostly the coarse aerosol mode and are of relevant interest for the atmospheric radiative balance [13],[14], [15].

Extreme episodes of aerosol load over the European continent and especially over the Mediterranean region are often related to Saharan dust intrusions [16],[17],[18], [19], [20][21], [22], [23], [14], [24],[25]. Saharan Desert affects also the Balkan Peninsula [26],[27], [28], [29], [30], [31], [32], [33]. However, its eastern side, the region in which is situated also Albania, is affected also by the Arabian Desert [25]. Continuous studies regarding atmospheric over the Albanian region have been performed during the last years [34], [35].

The paper consists of the study spatial and temporal distribution of aerosol loads and the special case of two intense dust events.

MATERIALS AND METHODS

To investigate dust concentrations, several methodologies may be implied. Among them, the most utilized methods are; in-situ measurements such are in-situ observations, passive and active remote sensing, satellite products, modelling, etc. Thus, the model output may be used in the space regions and time intervals which lack of measurement data.

To investigate dust intrusions over the region of Albania, satellite observations and model databases are used. Satellite observations are provided by the Moderate Resolution Imaging Spectroradiometer (MODIS) https://ladsweb.modaps.eosdis.nasa.gov/, on-board of the Aqua and Terra satellites. Moreover, GIOVANNI tool (Earth Data) is used to provide the statistics of the AOD data (https://giovanni.gsfc.nasa.gov/giovanni/).

The investigation of the dust intrusions is based on the identification of the variability of their principal optical and microphysical properties; aerosol optical depth (AOD), Angstrom exponent (AE), etc. This study aims to investigate dust intrusions over a 19-year period; February 2000 – February 2019.
EOSDIS Worldview which provide images based on the Corrected Reflectance layer, are used to show the presence of dust plumes over the region under investigation [36].
Furthermore, model products, such are Hybrid Single Particle Lagrangian Integrated Trajectory model – HYSPLIT [37], [38], [39] and Navy Aerosol Analysis Prediction System – NAAPS [40] are engaged in forecasting air mass movement and identification of aerosol sources.

RESULTS AND DISCUSSION

Spatial and temporal distribution of aerosol loads

Aerosol Optical Depth (AOD) and Angstrom Exponent (AE) are the principal aerosol optical parameters taken into account in this investigation. AOD_{550} provided by the MODIS, maps the aerosol load distribution over Albania region, give inter-annual trend and seasonal variation of the AOD mean values. AOD_{550} map over the Albanian region is presented in Fig. 1.

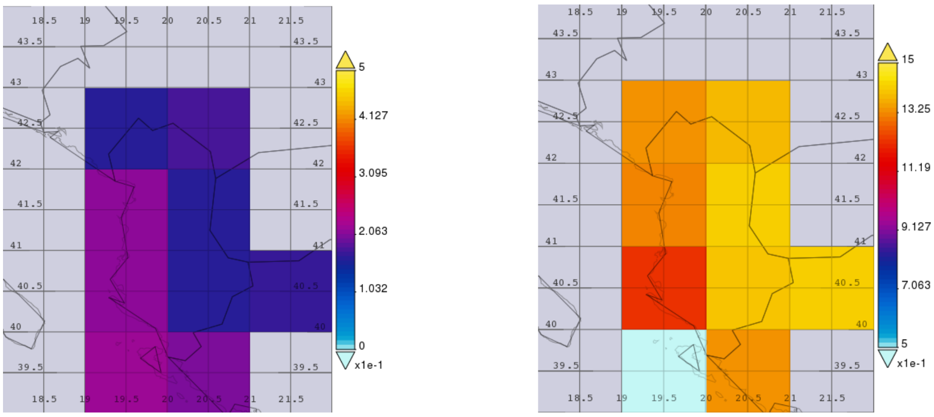

Fig. 1 Time Averaged Map of AOD_{550} and Deep Blue Angstrom Exponent for land (0.412-0.47 micron): Mean of Daily Mean monthly 1 deg. [MODIS-Terra MOD08_M3 v6.1], period Feb2000-Mar2020.

The map of the Fig.1 suggests that the highest aerosol load was found over the southwestern and western parts of Albania (AOD_{550}=0.21 and AOD_{550}=0.23), associated by the lowest Angstrom Exponent ($AE_{412-470}$=1.2 and $AE_{412-470}$=1.3). The eastern and northwestern part of Albania has the lowest aerosol load (AOD_{550}=0.15) associated by Angstrom Exponent ($AE_{412-470}$=1.5 and $AE_{412-470}$=1.4). Meanwhile the other parts of the region have intermediate values of AOD. However, the mean values of AOD don't differ too much, because the relatively small area under the investigation. In order to have more insight that the simple total average of AOD_{550}, time series of their monthly averaged values and inter-annual variations of their seasonal means are presented in Fig. 2.

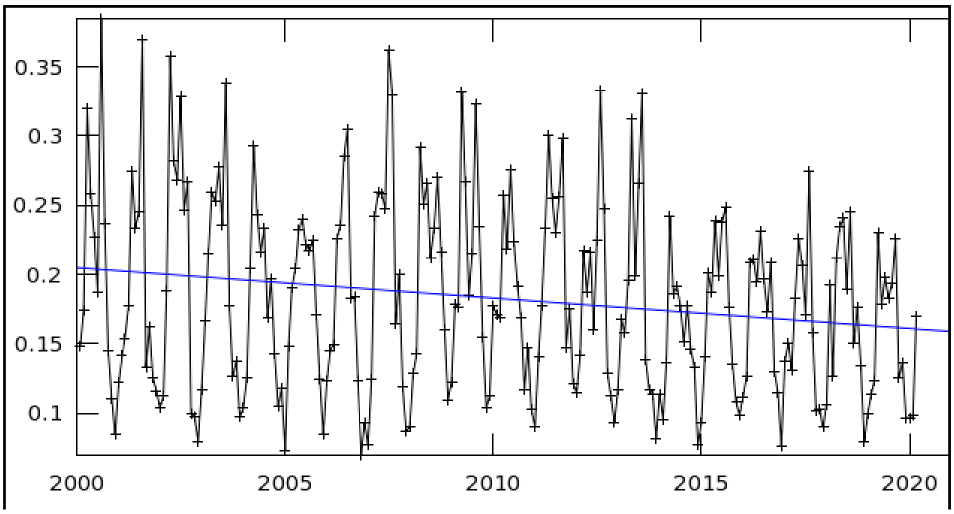

a)

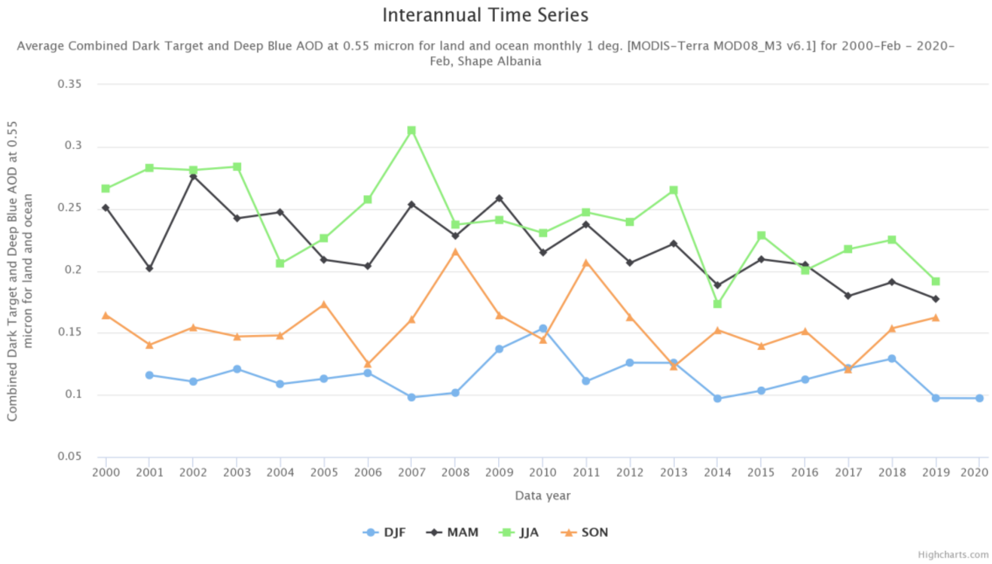

b)

Fig. 2. a) Time series of monthly-averaged AOD_{550}. b) Inter-annual time series of the seasonal means AOD_{550}. Combined Dark Target and Deep Blue for land and ocean; period Feb 2000–Feb 2019

The upper graph of the Fig. 2 suggests a cyclic variation of the mean AOD_{550} over the region. This pattern is investigated further during the seasonal distribution of AOD. The lower graph of the Fig.2 presents inter-annual variation of the regional mean of seasonal AOD_{550} data. Although there are not evidenced any clear trend, a maximum was observed during the period 2007-2008, especially during the summer of 2007. Seasonal maps of AOD_{550} presented in Fig. 3 are used to identify the most affected areas by aerosol load during each season.

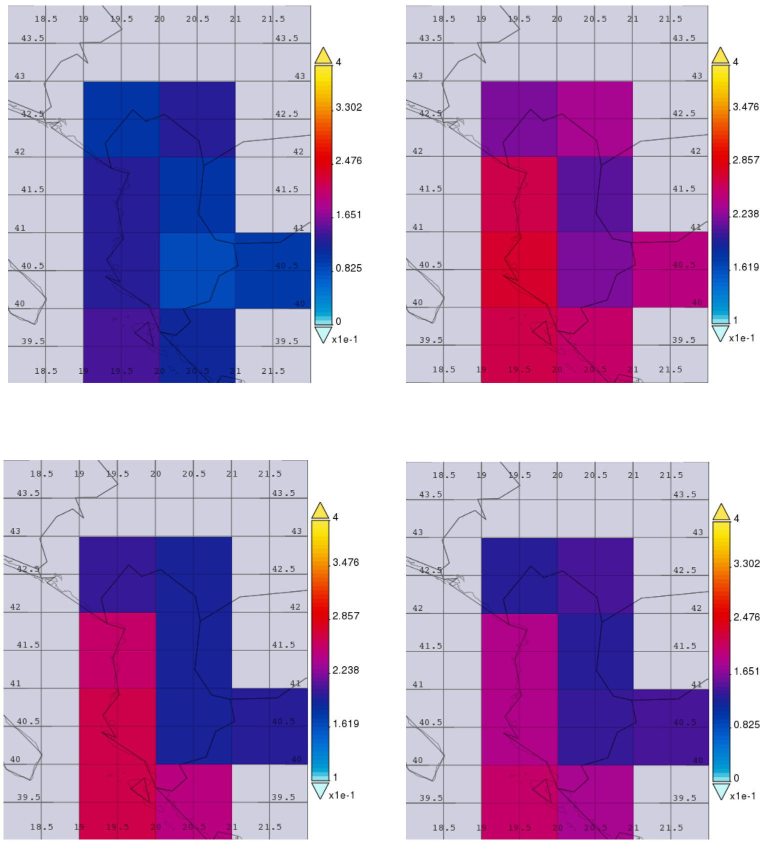

Fig. 3 Seasonal distribution of the regional AOD_{550}; period DJF (upper-left), JJA (upper-right), MAM (lower-left) and SON (lower-right), 2000-2020. Average Combined Dark Target and Deep Blue AOD at 0.55 micron for land and ocean monthly 1 deg. [MODIS-Terra MOD08_M3 v6.1] for SON months 2000- 2020, Shape Albania

The highest aerosol load in terms of AOD is observed during summer and spring; JJA (AOD_{550}=0.22÷0.30) and MAM (AOD_{550}=0.20÷0.27). Much less aerosol loads are observed during the rest of the year; autumn and especially during winter; SON (AOD_{550}=0.12÷0.19) and DJF (AOD_{550}=0.03÷0.15).

In order to give more insights over the aerosol types during the aerosol loads, the Angstrom Exponent $AE_{412-470}$ is used. This parameter is higher for fine-mode aerosols and lower for the coarse-mode aerosols. Same, as in Fig. 2.b inter-annual time series of the seasonal means of $AE_{412-470}$ are presented in Fig.4.

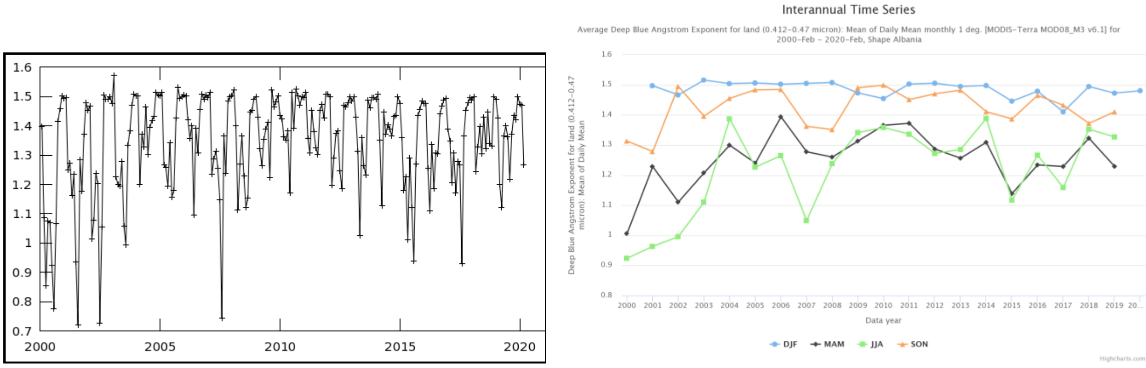

Fig. 4 Inter-annual time series of the $AE_{412-470}$. Mean of daily mean 1deg. MODIS-Terra MOD08_M3 v6.1, Feb2000–Mar2020

Fig. 2.b suggests that aerosol load is more intense during MAM-JJA (0.2-0.3), while DJF is the least affected by aerosol load (0.10-0.15). On the other hand, Fig.4 suggests that AE takes the lowest values (1.1-1.4) during the period JJA-MAM. It has got 1.3-1.5 during SON and the highest values (around 1.5) during DJF. Thus, the AOD and AE values are negatively correlated, suggesting that the presence of the coarse mode. The highest aerosol load composed by coarse mode aerosols (AOD_{550}=0.32 and $AE_{412-470}$=1.05) during JJA 2017, suggest an intense mineral dust event during that period. However, values of AE higher than 1.0 suggest a mixing state of coarse and fine particles. Thus, the AE values indicate that aerosol isn't pure dust, but mixed with fine mode aerosols, depending on the pathway of the air masses. Mean AE values are almost uniformly distributed over the whole territory. However, during the most active seasons, summer and spring, the southwestern region shows clear lower AE values; 0.3 on JJA and 0.8 in MAM. This fact suggests that this sector is more affected by the coarse mode aerosols compared to the remaining part of Albania (Fig.5).

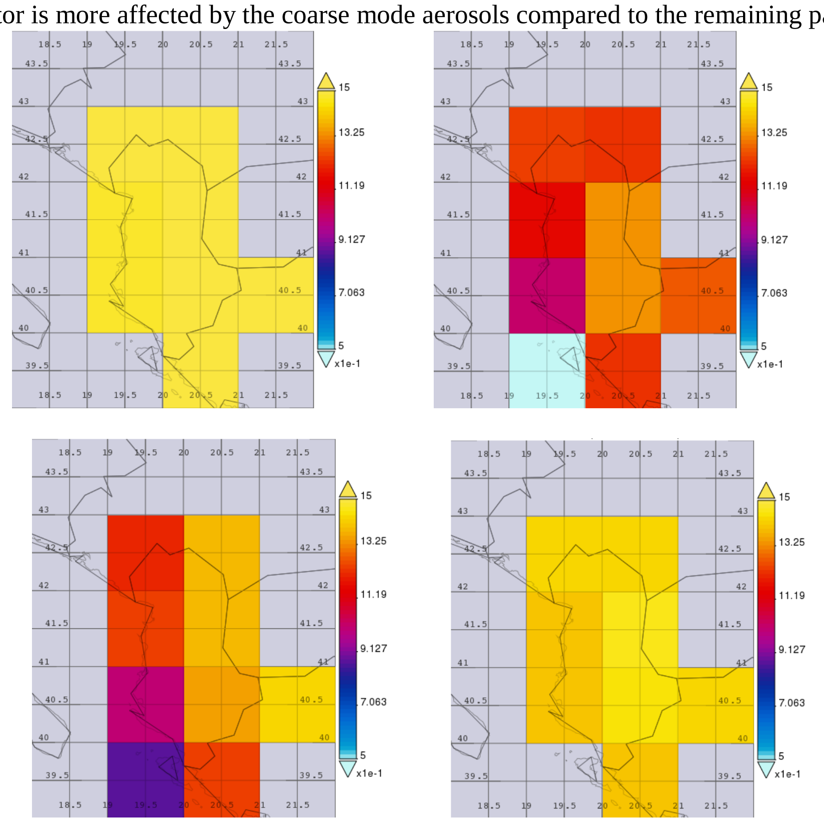

Fig. 5 Seasonal distribution of the regional $AOD_{412-470}$; period DJF (upper-left), JJA (upper-right), MAM (lower-left) and SON (lower-right), 2000-2020. Average Combined Dark Target and Deep Blue AOD at 0.55 micron for land and ocean monthly 1 deg. [MODIS-Terra MOD08_M3 v6.1] for SON months 2000- 2020, Shape Albania

An overall estimation of the optical characteristics of the aerosols, both AOD and AE, is given also by analysing their statistical distributions.

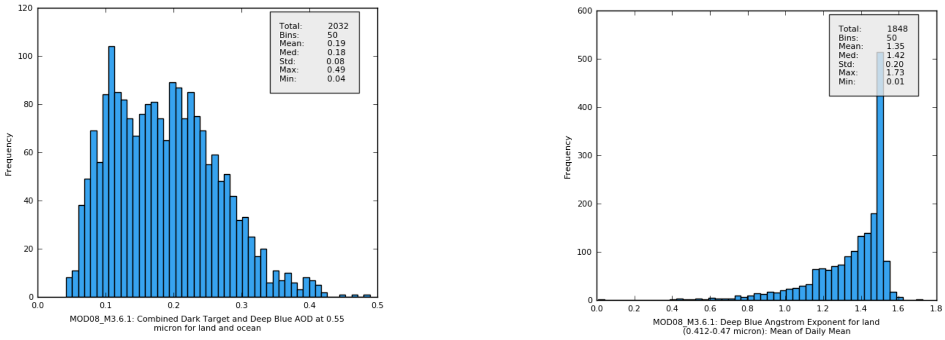

a) b)

Fig. 6 Statistical distribution of the AOD_{550} and $AE_{412\text{-}470}$ values. MODIS-Terra MOD08_M3 V6.1, Feb 2000 – Feb 2019.

Statistical data of AOD_{550} ranges in the interval 0.04-0.49, with a mean value of 0.19±0.08 (Fig.6). This is a considerable value, indicating a continuous presence of aerosol load over the region. While, $AE_{412\text{-}470}$ ranges over the interval 0.01-1.73, with a mean value of 1.35±0.20. This value suggests domination of the fine mode aerosols but also the presence of the mixed phase. The coefficients of variation of AOD_{550} and $AE_{412\text{-}470}$ are 42.1% and 14.8% respectively. The last result suggests that aerosol optical depth values are more dispersed than those of Angstrom exponent.

Characteristics of the most intense dust events

The most intensive dust events in terms of aerosol optical depth were evidenced tracking information from GIOVANNI. The maxima of AOD_{550} during the entire period 2000-2019 indicate the most intense dust events over the Albania region (Fig.7).

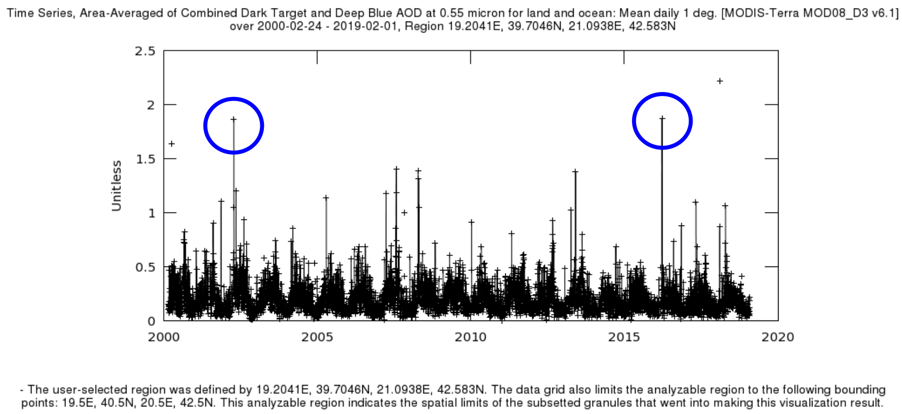

Fig. 7 Identification of two of the most intense dust events in terms of AOD_{550}; IDE-I and IDE-II.

Annual variation of AOD_{550} during the two years with intense events 2002 and 2016, detect the exact time-occurrence of these events. Thus, Fig. 8-9 suggest that the two most intense dust events occur on 13Apr02 (IDE-I) and 23Mar16 (IDE-II).

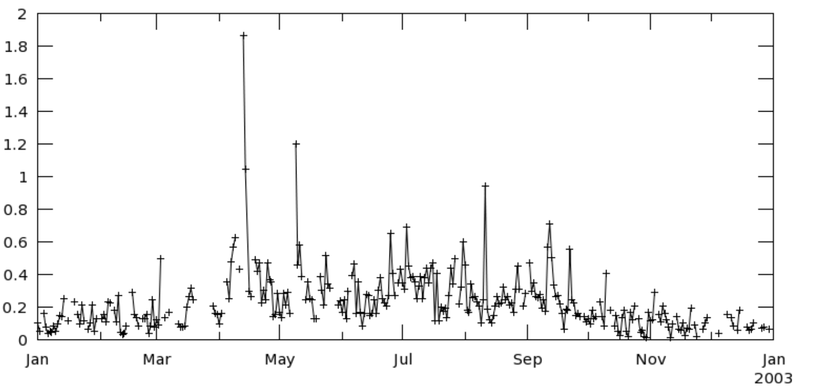

Fig. 8 Variation of AOD_{550} during the period Jan 2002 – Dec 2002. Identification of the IDE-I.

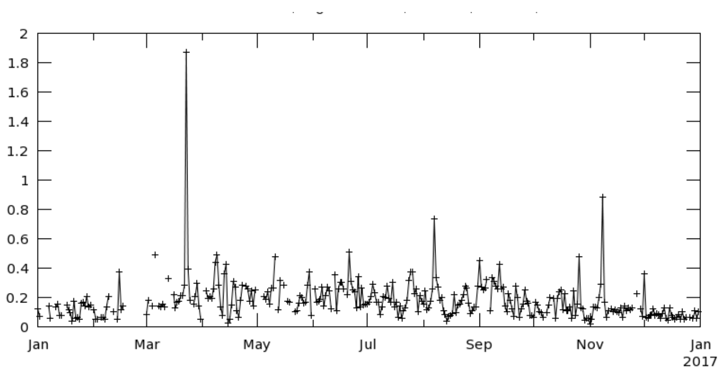

Fig. 9 Variation of AOD_{550} during the period Jan 2016 – Dec 2016. Identification of the IDE-II.

Additionally, images of EOSDIS during these two days are presented in Fig. 10.

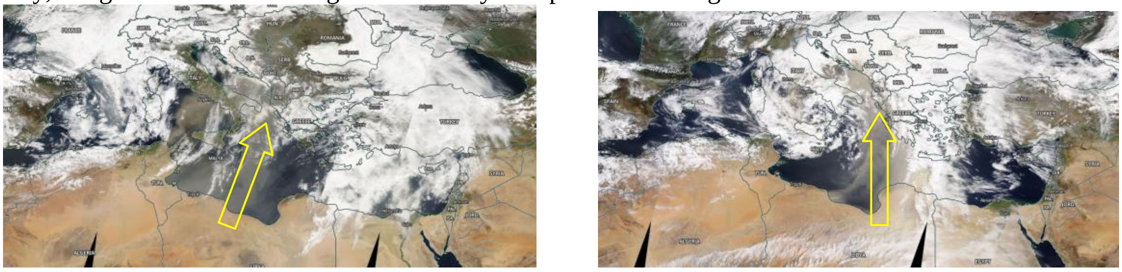

a) b)

Fig. 10 Dust plumes over the area under investigation. a) First intense dust event 13Apr02, b) second intense dust event 23Mar16. MODIS-Terra Corrected Reflectance.

According to the images of Fig.10, in both cases, dust plumes originate from Saharan Desert and enter the Albanian region from its southwestern part. The dust originates in the first event from Libya-Tunisia region, while in the second event dust originate more easterly (Libyan region). The pathways of air masses during these events are more detailed analysed using the HYSPLIT model Fig. 11. a.

As Fig.10 suggested, also Fig.11 show 72hr HYSPLIT back-trajectories of air masses originating over the Libyan-Tunisian region. Furthermore, the NAAPS maps show the intense dust intrusion overpassing the entire Balkan Peninsula coming from Libyan Desert. Despite of this, a significative presence of sulphate over this region is forecasted during the second event. No smoke contamination is forecasted by the NAAPS model for both dust events. According to the HYSPLIT back-trajectories, air masses seem to bring on more dust during the IDE-I compared to the IDE-II. This is justified because while during the IDE-I air masses overpassing Albania at the altitudes 4-6 km pass through Saharan Desert at low altitudes which enabled them to be effective in collecting dust. On the other hand, during the IDE-II, only air masses overpassing Albania at 4 km altitudes can potentially collect dust over Saharan Desert.

In short, main characteristics of IDE-I and IDE-II are respectively as follow; Combined Dark Target and Deep Blue land and ocean (MOD08_M3_V6.1) AOD_{550} both 1.8, Deep Blue Angstrom Exponent for land (MOD08_M3_V6.1) $AE_{412\text{-}470}$ 1.8 and 0.9, dust scattering AOT_{550}(PM1) from MERRA II are 0.43 and 0.41.

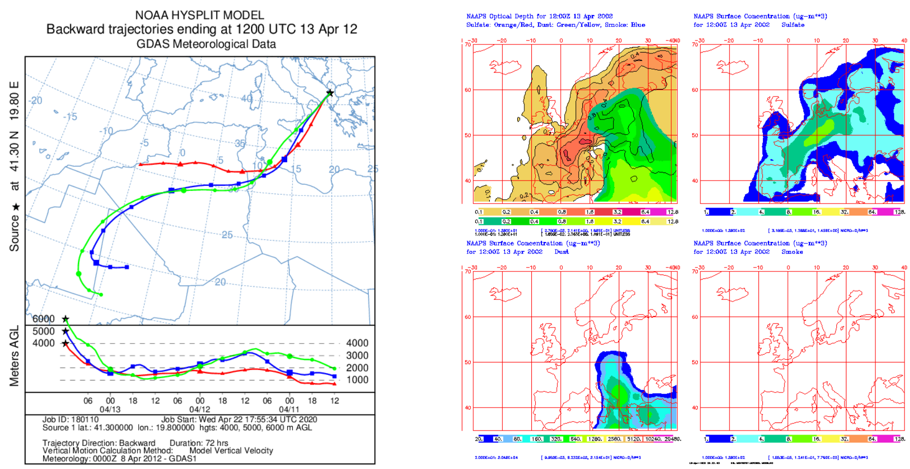

a) b)

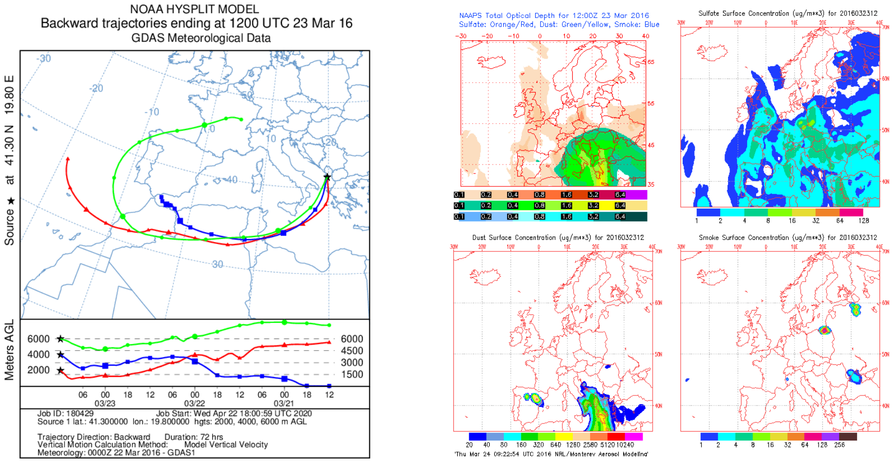

c) d)

Fig. 11 a) HYSPLT 72hr back-trajectories and NAAPS maps over Europe during the two intense dust events. a-b) IDE-I and c-d) IDE-II

CONCLUSION

In this paper a study about the dynamics of the variations of the principal aerosol optical parameters over Albania region is presented. Principal aerosol parameters taken into analysis, here are aerosol optical depth and Angstrom exponent.

Southwestern and western regions of Albania are the most affected by aerosol loads. However, the southwestern part was mainly influenced by the coarse mode, while the remaining area is dominated by the fine mode aerosols, or at least by mixed aerosols. No inter-annual trend was observed for AOD and AE values. Moreover, a maximum of AOD was observed during the period 2007-2008. The most active period characterized by higher aerosol loads is the period spring-summer. Maximal values of aerosol load were observed during the summer season (AOD550=0.22÷0.30) and spring season (AOD550=0.20÷0.27). The significantly lower aerosol load was observed during autumn (AOD550=0.12÷0.19) and even less during winter (AOD550=0.03÷0.15).

Two intense dust events were detected analysing the AOD data; in April 2002 and March 2016. During these two events, averaged zonal mean AOD550 reached high values as 1.8, whereas dust scattering AOT550(PM1) goes up to 0.4.

Acknowledgements

Analyses and visualizations used in this paper were produced with the Giovanni online data system, developed and maintained by the NASA GES DISC. We also acknowledge the MODIS mission scientists and associated NASA personnel for the production of the data used in this research effort. The authors gratefully acknowledge the NOAA Air Resources Laboratory (ARL) for the provision of the HYSPLIT transport and dispersion model and/or READY website (https://www.ready.noaa.gov) used in this publication.

REFERENCES

[1]. V. Ramanathan, P, J, J. Crutzen, T and e. a. Kiehl, "Aerosols, climate, and the hydrologicalcycle," Science, 294,, p. 2119–2124, 2001.

[2]. B. Gantt, J. Xu, N. Meskhidze, Y. Zhang, A. Nenes, S. J. Ghan, X. Liu, R. Easter and R. Zaveri, "Global distribution and climate forcing of marine organic aerosol," in Part 2: Effects on cloud properties and radiative forcing, Atmos; Chem; Phys;, 2012, pp. 12, 6555–6563.

[3]. T. Stocker, F, D. Qin, G. Plattner,. K, M. Tignor, S. Allen, K, J. Doschung, A. Nauels, Y. Xia, V. Bex, P. and Midgley and M, "IPCC: Fifth Assessment Report: Climate Change (2013); The Physical Science Basis, Contribution of Working Group I to the Fifth Assessment Report of the Intergovernmental Panel on Climate Change," Cambridge University Press, 2013.

[4]. O. Altaratz, Koren, I, Remer, L and Hirsch, E, "Cloud invigoration by aerosols-coupling between microphysics and dynamics," Atmos, pp. 140, 38–60, 2014.

[5]. Rosenfeld, D;, "Aerosol-cloud precipitation interactions. Part 1," in The nature and sources of cloud-active aerosols, 2008, pp. 89, 13–41.

[6]. G. Lenderink, A. van Ulden, v. M. E and v. d. H. B, "Summertime inter-annual temperature variability in an ensemble of regional model simulations: analysis of the surface energy budget," Clim Change, p. 81:233–47, 2007.

[7]. D. Shindell, J. Kuylenstierna, C, I, E. Vignati, R. van Dingenen, M. Amann, Z. Klimont, S. Anenberg, C, N. Muller, G. Janssens-Maenhout, F. Raes, J. Schwartz, G. Faluvegi, L. Pozzoli, K. Kupiainen, L. Höglund-

Isaksson, L. Emberson, D. Streets and Ramanathan, "Simultaneously mitigating near-term climate change and improving human health and food security," Science, 335, p. 183–189, 2012.

[8]. D. Dockery, W, C, A, X. Pope III and e. a. Xu, "An association between air pollution and mortality in six US cities," New England, 1993.

[9]. L. Perez, A. Tobias, X. Querol, N. Kunzli, J. Pey, A. Alastuey, M. Viana, N. Valero, M. Gonzalez-Cabre and J. and Sunyer, "Coarse particles from Saharan dust and daily mortality," Epidemiology, 19,, p. 800–807, 2008.

[10]. Karanasiou, N. Moreno, T. Moreno, M. Viana, F. de Leeuw and X. and Querol, "Health effects from Sahara dust episodes in Europe," Literature review and research gaps, Environment Int, pp. 47, 107–114, doi:10;1016/j;envint;2012;06;012;, 2012.

[11]. G. Kallos, M. Astitha, P. Katsafados and C. and Spyrou, "Long-range transport of anthropogenically and naturally produced particulate matter in the Mediterranean and North Atlantic: Current state of knowledge," Journal of Appl; Meteorol; Climatol;, pp. 46, 1230– 1251;, 2007.

[12]. P. Ginoux, J. Prospero, T. Gill, N. Hsu and M. Zhao, "Global scale attribution of anthropogenic and natural dust sources and their emission rates based on modis deep blue aerosol products," Geophys, p. 50, 2012.

[13]. P. Nabat, S, M. Somot, M. Mallet, F. Michou, F. Sevault, D. Driouech, A. Meloni, C. di Sarra, P. Di Biagio, M. Formenti, J. Sicard, -F, a. M. Léon, N and Bouin, "Dust aerosol radiative effects during summer 2012 simulated with a coupled regional aerosol–atmosphere–ocean model over the Mediterranean," Atmos; Chem; Phys; 15, p. 3303–3326, 2015.

[14]. F. Mandija, J.-L. Guerrero-Rascado, H. Lyamani, M. J. Granados-Muñoz, Alados-Arboledas and L, "Synergic estimation of columnar integrated aerosol properties and their vertical resolved profiles in respect to the scenarios of dust intrusions over Granada," Atmospheric Environment, pp. 145, 439-454, 2016.

[15]. Gkikas, V, C. Obiso, P, O. García-Pando, N. Jorba, L. Hatzianastassiou, S. Vendrell, S. Basart, S. Solomos, a. J. Gassó, M and Baldasano, "Direct radiative effects during intense Mediterranean desert dust outbreaks," Atmos; Chem; Phys;, vol. 18, p. 8757–8787, 2018.

[16]. H. Lyamani, F. Olmo, J, A. Alcantara and L. Alados-Arboledas, "Atmospheric aerosols during the 2003 heat wave in southeastern Spain II: microphysical columnar properties and radiative forcing," Atmos; Environ, pp. 40, 6465–6476, 2006.

[17]. X. Querol, A. Alastuey, J. Pey, M. Cusack, N. Pérez, N. Mihalopoulos, C. Theodosi, E. Gerasopoulos, N. Kubilay and M. Kocak, "Variability in regional background aerosols within the Mediterranean," Atmos; Chem; Phys; 9, p. 4575–4591, 2009.

[18]. J. Guerrero-Rascado, L, F, J, I. Olmo, F. Avilés-Rodríguez, D. Navas-Guzmán, H. Pérez-Ramírez, a. L. Lyamani and A. Arboledas, "Extreme Saharan dust event over the southern Iberian Peninsula in september 2007: active and passive remote sensing from surface and satellite," Atmos; Chem; Phys, pp. 9, 8453-8469, 2009.

[19]. Ansmann, M. Tesche, P. Seifert, S. Groß, V. Freudenthaler, A. Apituley, K. M. Wilson, I. Serikov, H. Linné, B. Heinold, A. Hiebsch, F. Schnell, J. Schmidt, I. Mattis, U. Wandinger and M. Wiegner, "Ash and fine-mode particle mass profiles from EARLINET-AERONET observations over central Europe after the eruptions of the Eyjafjallajökull volcano in 2010," Geophys, p. 116, 2011.

[20]. Ansmann, D. Althausen, T. Kanitz, R. Engelmann, A. Skupin, H. Baars, A. Klepel, M. Haarig, B. Heinold, I. Tegen, C. Toledano, D. Prescod and D. Farrell, "Saharan dust longrange transport: SALTRACE lidar observations at Barbados and aboard RV Meteor (Guadeloupe to Cape Verde) versus dust transport modelling," in DUST 2014 – International Conference on Atmospheric Dust, Castellaneta Marina, Italy, 2014.

[21]. Papadimas, D, N. Hatzianastassiou, C. Matsoukas, M. Kanakidou, N. Mihalopoulos and I. Vardavas, "The direct effect of aerosols on solar radiation over the broader Mediterranean basin," Atmos; Chem; Phys; 12, p. 7165–7185, 2012.

[22]. Gkikas and a. et, "The regime of intense desert dust episodes in the Mediterranean based on contemporary satellite observations and ground measurements," Atmos; Chem; Phys, pp. 13, 12135–12154, 2013.

[23]. E. Marinou, V. Amiridis, I. Binietoglou, A. Tsikerdekis, S. Solomos, E. Proestakis, D. Konsta, N. Papagiannopoulos, A. Tsekeri, G. Vlastou, P. Zanis, B. Balis, U. Wandinger and A. Ansmann, "Three-dimensional evolution of Saharan dust transport towards Europe based on a 9-year EARLINET-optimized CALIPSO dataset," Atmos; Chem; Phys; 17, p. 5893–5919, 2017.

[24]. F. Mandija, M. Sicard, C. A, L. Alados-Arboledas, J.-L. Guerrero-Rascado, R. Barragan, J.-A. Bravo-Aranda, M.-J. Granados-Muñoz, H. Lyamani, C.-M. Porcar, F. Rocadenbosch Burillo, A. Rodríguez, A. Valenzuela and D.-G. Vizcaíno, "Origin and pathways of the mineral dust transport to two Spanish EARLINET sites: effect on the observed columnar and range-resolved dust optical properties," Atmospheric Research, pp. 187, 69-83, 2017.

[25]. F. Mandija, V. Chavez Perez, R. Nieto, M. Sicard, V. Danylevsky, J.-A. Anel Cabanelas and L. Gimeno, "The climatology of dust events over European continent using data of the Dust Regional Atmospheric Model," Atmospheric Research, pp. 209, 144-162, 2018.

[26]. Balis, V. Amiridis, S. Kazadzis, A. Papayannis, G. Tsaknakis, S. Tzortzakis, N. Kalivitis, M. Vrekoussis, M. Kanakidou, N. Mihalopoulos, G. Chourdakis, S. Nickovic, C. Perez, J. Baldasano and M. Drakakis, "Optical characteristics of desert dust over the East Mediterranean during summer: A case study, Ann," in Geophys, 2006.

[27]. Kaskaoutis, G, p. Kosmopoulos, H. Kambezidis, D, P. Nastosc and T, "Aerosol climatology and discrimination of different types over Athens, Greece, based on MODIS data," Atmospheric Environment, pp. 41 (34), 7315-7329, 2007.

[28]. L. Labzovskii, F. Toanca, Nicolae and D, "Determination of Saharan dust properties over Bucharest, Romania part 2: study cases analysis," Phys; Vol; 59, pp. 9–10, 1097–1108, 2014.

[29]. Urlea, A. Boscornea, S. Nicolae Vâjâiac, F. Ţoancă, N. Barbu, S. Ştefan and I. Bunescu, "Studies of Saharan dust intrusions over Bucharest Using ceilometer's measurements and satellite data," EPJ Web of Conferences 176, p. 11004, 2018.

[30]. N. Hatzianastassiou, M. Gavrouzou, A. Gkikas and N. Mihalopoulos, "A climatology of desert dust aerosols over the Mediterranean basin based on contemporary satellite data," Geophysical Research Abstracts Vol; 21, pp. EGU2019-11479, 2019.

[31]. Mandija, F. Vila, E. Lukaj, Bushati and J, "Desert dust episodes over Balkan Peninsula," in Proceedings of the 10th Balkan Physical Union, 2019.

[32]. Dundar, "Investigation of the sand and dust storms over greater Mediterranean basin and determination of the dust source areas affecting Turkey," in Doctoral Thesis, Turkey, Hacette University, Dept; of Environmental Engineering, 2019.

[33]. Kaskaoutisa, G, A. Rashkib, U. Dumkac, C, A. Mofidid, H. Kambezidisa, D, B. Psilogloua and E, "Atmospheric dynamics associated with exceptionally dusty conditions over the eastern Mediterranean and Greece in March 2018," Atmos;Res;, pp. 218 (1) 269-284;, 2019.

[34]. Mandija and F. Vila, "Seasonal Cycles of Atmospheric Ion and Aerosol Concentrations in an Urban Area," International Journal of Scientific Research in Environmental Sciences (IJSRES), 1(7), pp. 132-137, 2013.

[35]. F. Mandija, "Characteristics, spatial distributions and main aerosol sources around the area of Shkodra Lake," Int; J; Continuing Engineering Education and Life-Long Learning, p. 259–273, 2015.

[36]. L. Gumley and J. a. S. J. Descloitres, "NASA Earthdata - Creating Reprojected True Color MODIS Images," in A Tutorial; Version 1;0;2, NASA, 2010.

[37]. F. Stein, R. R. Draxler, G. D. Rolph, B. J. B. Stunder, M. D. Cohen and F. Ngan, "NOAA's HYSPLIT atmospheric transport and dispersion modeling system," Bull; Amer; Meteor; Soc; 96, pp. 2059-2077, 2015.

[38]. Rolph, A. Stein and B. and Stunder, "Real-time Environmental Applications and Display system: READY," Environmental Modelling & Software, 95, pp. 210-228, 2017.

[39]. M. Micheletti, I, K. Louedec, M. Freire, a. et, Eur, Phys, J and Plus, "Aerosol concentration measurements and correlations with air mass trajectories at the Pierre Auger Observatory," p. 132: 245, 2017.

[40]. P. Lynch, J. Reid, S, D. Westphal, L, J. Zhang, T. Hogan, F, E. Hyer, J, C. Curtis, A, D. Hegg, A, Y. Shi, J. Campbell, R, J. Rubin, I, W. Sessions, R, F. Turk, J, A. and Walker and L, "An 11-year global gridded aerosol optical thickness reanalysis for atmospheric and climate sciences," Geosci; Model Dev, pp. 9, 1489– 1522;, 2016.